Partial and Full Interaction Behaviour of CFRP Plated Steel Member Due to The Yielding of Steel

Ibrisam Akbar
Department of Civil Engineering
Universiti Teknologi PETRONAS
Bandar Seri Iskandar
31750 Tronoh, Perak,
Malaysia
ibrisam_akbar@petronas.com.my

Deric J Oehlers, Mohamed Ali Sadakkathulla
School of Civil Environmental and Mining Engineering,
Faculty of Engineering, Computer & Mathematical Sciences
Level 1, Ingkarni Wardli
The University of Adelaide SA 5005
Australia

Abstract— **The reliability of the strengthening of Fibre Reinforced Polymer (FRP) to steel or concrete structures depends on the success of the stress transfer between the FRP plate and steel or concrete element. In order to simulate the stress transfer, a simple numerical approach was developed, employing the partial interaction theory. In this paper, the numerical method applying the partial interaction theory is used to evaluate the debonding of FRP plated steel member due to the yielding of steel. An accurate local bond-slip (τ-δ) model was adopted in the numerical procedure. A set of pull test specimen was tested to prove the existence of partial and full interaction regions along the bonded length. Comparison with the experimental and published results shows good correlations.**

Keywords; FRP, numerical, strengthening

I. INTRODUCTION

Carbon Fibre Reinforced Polymer (CFRP) is a material of choice in the strengthening and rehabilitation of structures mainly because of its ease of use. The high stiffness-to-weight and strength-to-weight ratios of CFRP combined with the superior environmental durability has made them so appealing to be used (Buyukozturk et al. 2003). However, the reliability of the strengthening of CFRP to steel or concrete structures depends on the success of the stress transfer between the CFRP plate and steel or concrete element (Al-Saidy et al. 2005; Sebastian 2003b) and the first critical stage is to understand the bond-slip characteristics of CFRP plated steel members which is susceptible to the yielding of the steel.

A. Bond-slip relationship

The bond-slip relationship plays an important role in characterising the behaviour of CFRP bonded steel members. It can be used to derive the bond strength, the slip, and the effective bond length. Conventionally, the derivation of the bond-slip relationship was carried out experimentally in pull tests. Strain gauges were glued on the CFRP plate along the bond length from which the values of the bond stress could be calculated from the strain readings. The slip can be determined by integrating the measured strain distribution along the plate length (Xia and Teng 2005). A bilinear shape is considered to be a reasonable idealisation of the bond-slip relationship for both concrete and steel members glued with CFRP (Xia and Teng 2005; Yuan et al. 2004; Zhao and Zhang 2007). Fig. 1 shows the bilinear bond-slip relationship which consists of the maximum bond stress, τ_{max}, the maximum slip, δ_{max} and the slip at the maximum bond stress, δ_1. The area encompassed by the bond-slip relationship is the fracture energy, G_f. So long as the values of τ_{max} and δ_{max} are constant, the value of G_f does not change since the area under it does not change. For example, the unilinear relationship has the same value of τ_{max} and δ_{max} which resulted the same area underneath similar to that of the bilinear relationship.

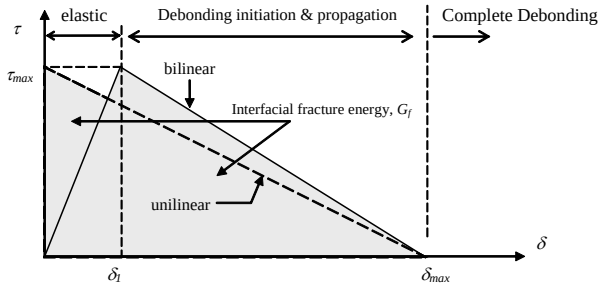

Figure 1. Bilinear bond-slip relationship

B. Pull test

An experimental research was conducted to test 13 numbers of CFRP-to-steel specimens to measures the bond-slip behaviour by varying the adhesive thickness and adhesive types (Xia and Teng 2005). The test specimens consist of a steel block bonded with CFRP plates as shown in Fig. 2. Strain gauges were attached along the CFRP at spacings with a range from 25 mm to 50 mm. The shear stresses along the CFRP were calculated from the readings of the strain gauges so they represent the average shear stress upon the intervals of each strain gauge. However, this process was exhaustive and costly. Furthermore, the strain gauges can only give average stresses

over the strain gauge length and can miss the peak stresses. The readings may be affected by local distortion of the plate whilst debonding since the strain gauges are only placed on the outer surface of the CFRP plate. The improvement in obtaining the τ-δ relationship using structural mechanics method was conducted (Akbar et al. 2010b). Similar test was conducted on concrete material (Haskett et al. 2007), however using steel, the problem of violent variations in the strain readings in the CFRP-concrete experiment can be eliminated (Zhao and Zhang 2007).

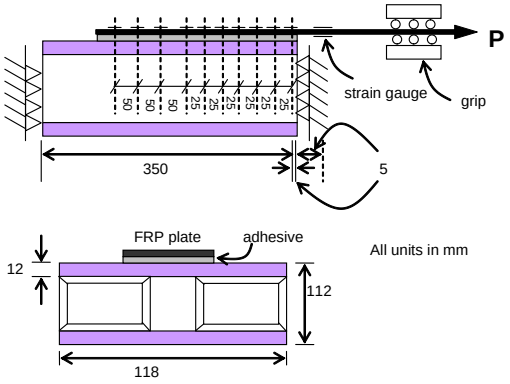

Fig. 2 Pull test specimen.

It was shown from the previous research by (Al-Emrani and Kliger 2006) on CFRP plated steel loaded axially as shown in Fig. 3(a) was that debonding may occurs at the plate end and at the middle where the steel has yielded. The existence of high bond stress, initially at the plate end and at the middle section once the steel has yielded as shown in Fig. 3 (b) simulates one of the debonding possibilities in a steel beam strengthened with CFRP. Another important feature to observe from the finite element analysis was the existence of full interaction region between the high bond stress regions indicated by the near 0 bond stress shown in Fig. 3 (b). The significance of this finding was that the full interaction region is not critical and does not need as much attention as the plate end and middle regions. Consequently it may affect on how CFRP is used for the strengthening of steel members.

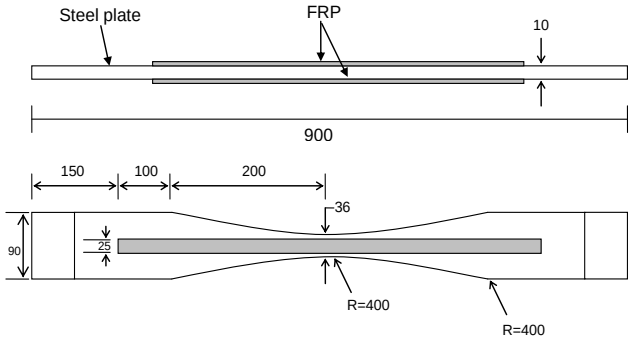

(a) Test specimen

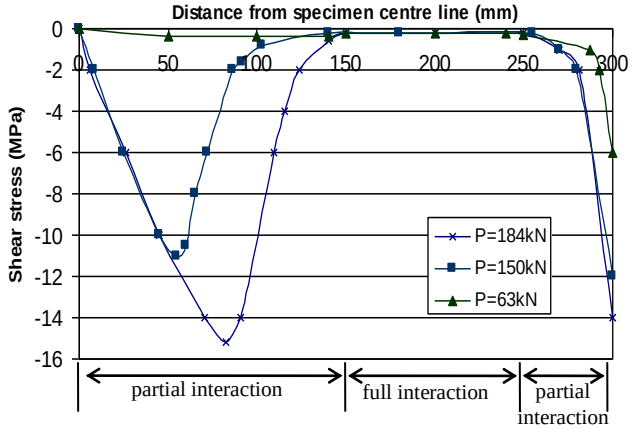

(b) Finite element stress distributions

Figure 3 Specimen and finite element results (Al-Emrani and Kliger 2006)

II. PARTIAL INTERACTION THEORY

Consider the case of a composite beam in which the interface slip is totally prevented as in Fig. 4 such as the case of an CFRP plated steel member. The strain of the CFRP, ε_p is equal to the strain of the steel, ε_s. Hence, the slip strain, ds/dx, which is the difference of the two strains, ε_p and ε_s is 0. This condition is referred to full interaction. If the interface slip with some degree of friction is allowed to take place at the interface of the CFRP and steel as in Figure (b), the strains are no longer equal hence the slip strain, is no longer 0. This condition is known as partial interaction.

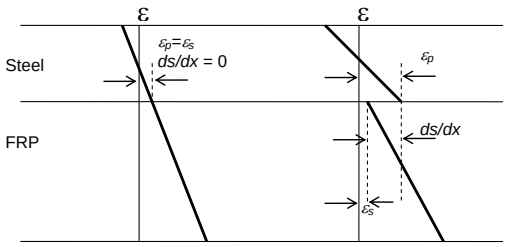

(a) full interaction (b) partial interaction

ISSN XXXX-XXXX

Figure 4. Degree of interaction

III. NUMERICAL METHOD

Consider a sample of steel plate with a constant width glued with CFRP as shown in Fig. 5 (a). Due to symmetry, the sample can be idealised as in Fig. 5 (b). Only half of the length is taken into consideration. The idealisation is develop to accommodate any local τ-σ relationship, failure plane (L_{per}) (Seracino et al. 2007), bonded length (L), cross section of the steel (A_s) and CFRP (A_p) and stress-strain profile of the steel plate and CFRP (which includes the Young's Modulus of the steel and CFRP, E_s and E_p respectively). The numerical procedures are as follows:

- Strain of steel is fixed at the middle $\varepsilon_s(0)$ and the strain of CFRP, $\varepsilon_p(0)$ is guessed.
- According to the stress-strain profile of the steel and CFRP, the load at the centre, $P_s(0)$ and $P_p(0)$ are calculated.
- The load in the steel and CFRP are calculated at the end of the first segment : $P_s(0)=\varepsilon_s E_s t_s L_{per}$ and $P_p(0)=\varepsilon_p E_p t_p b_p$.
- Due to symmetry at the centre, slip at this section is zero.
- The assumed slip at the centre corresponds to the local slip over the first segment length. Corresponding to this assumed slip, $\delta(0)$, the bond stress, $\tau(0)$, acting over the first segment length is calculated according to the local τ–δ relationship assumed.
- The bond force acting on the first segment is $B(0)=\tau(0)d_x b_b$.
- The load in the steel and CFRP is calculated at the end of the first segment : $P_s(1)=P_s(0)+B(0)$ and $P_p(1)=P_p(0)-B(0)$,
- The corresponding strain for the steel and CFRP are calculated: $\varepsilon_s(1)=\frac{P_s(1)}{(A_s E_s)}$ and $\varepsilon_p(1)=\frac{P_p(1)}{(A_p E_p)}$
- The slip strain is calculated: $\frac{ds(0)}{dx}=\varepsilon_s(0)-\varepsilon_p(0)$
- The change in slip over the first segment length is calculated by integrating the slip strain over the segment length: $\Delta s(0)=\int\frac{ds(0)}{dx}dx$.
- According to the change in slip over the segment length, the slip at the beginning of the second segment is calculated: $\delta(1)=\delta(0)-\Delta s(0)$.
- According to this slip the bond force acting over the second segment is calculated, with the numerical process repeating itself over the subsequent segments.
- If the boundary condition is not met, then change the assumed $\varepsilon_p(0)$.
- If the boundary condition is met, then increase the fixed $\varepsilon_s(0)$.

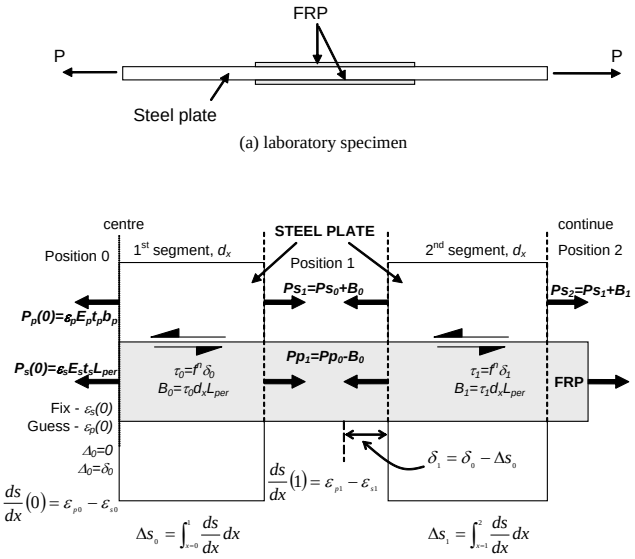

Figure 5. Graphical representation of the numerical analysis for CFRP plated steel members

IV. SPECIMEN PREPARATION AND TEST PROCEDURE

Fig. 6 shows the shape and dimension of the specimens which also consisted of two samples. This specimen was based on the experiment conducted previously in literature (Al-Emrani and Kliger 2006). The steel plates were tapered so that yielding of steel will occur on the middle section. The steel plate was varied in width from 100 mm at the widest and 30 mm at the thinnest. The constant width of 30mm that ran for 50 mm in length was designed to provide spaces for strain gauges. The CFRP that was bonded on to the steel plate was 250 mm long. However the first sample was bonded with one layer of CFRP and the other with two layers of CFRP. The thickness of CFRP plate is 1.2 mm.

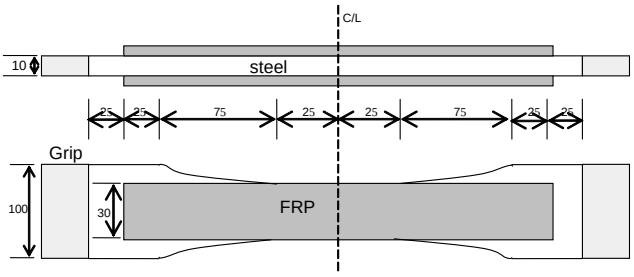

Figure 6. Shape and dimension of test specimen

The surfaces of the steel plate were sandblasted and cleaned with Acetone to remove any particles that may affect the bond between the steel and adhesive. The adhesive consisted of two parts; A and B which were mixed in the ratio of 1:1. After mixing, there was about 45 minutes for the adhesive to be applied on to the steel block before it became

ISSN XXXX-XXXX

too sticky to be workable. The adhesive was set to 1 mm thick. In order to achieve this, a 1 mm diameter ball bearing was placed along the steel block as spacers. After the CFRP plate was laid on the steel block, a sufficient force (a weight of 20 kg) must be placed on top of it for a minimum of five hours so that constant thickness of adhesive can be achieved and any excess adhesive out from the CFRP plate can be removed.

The specimen then was left for five days for curing. Subsequently, strain gauges were glued on the CFRP and steel surfaces to monitor the longitudinal strain at the middle section. Three tension pull tests were conducted on the steel plate to get the stress-strain relationship. The material properties are tabulated in Table 2. Finally, the specimen was tested on a Universal Testing Machine (UTM).

TABLE I. SPECIMEN PROPERTIES

Test specimen	Steel thickness, t_s (mm)	CFRP width, b_p (mm)	CFRP layer	Bonded length, L_p (mm)
VW 1	11.95	30.0	1	250
VW 2	11.96	30.0	2	250

TABLE II. MATERIAL PROPERTIES OF THE STEEL PLATE

Test specimen	Averaged
Yield load, P_y (kN)	115.9
Yield stress, f_y (MPa)	308
Yield strain, ε_Y	0.00152
Young's Modulus, E_s (MPa)	202348
Strain hardening stress, f_{sh} (MPa)	473
Strain hardening, ε_{sh}	0.078

V. TEST RESULTS AND DISCUSSIONS

Sample VW1 was bonded with a 125 mm CFRP on top and bottom faces of the steel plate as shown in Fig. 6, including all the numbering and locations of the strain gauges. Since the sample was symmetrical, the strain gauges were attached more on one side. However, the middle section was considered to be of importance hence the concentration of strain gauges attached is more.

Fig. 7 shows the specimen at failure. The debonding failures were a mix of steel-adhesive, CFRP-adhesive and CFRP layer. At the top surface as shown in Fig. 7 (a), the debonding failure occurred on the steel-adhesive layer at the middle part of the steel plate, whereas, CFRP-adhesive layer failure mainly occurred close to the plate end. At the bottom surface as shown in Fig. 7 (b), the debonding failure occurs at the steel-adhesive layer in the middle of the specimen, whereas, at the plate end debonding occurred at the CFRP-adhesive and within the CFRP layers as shown in Fig. 7 (b). The CFRP itself did not break. The steel plate breaks only after the CFRP has been totally debonded.

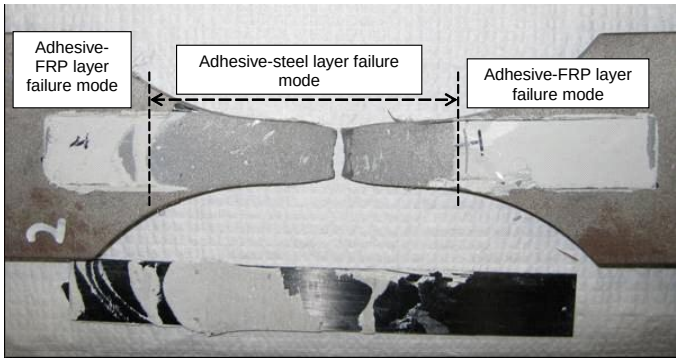

(a) top surface

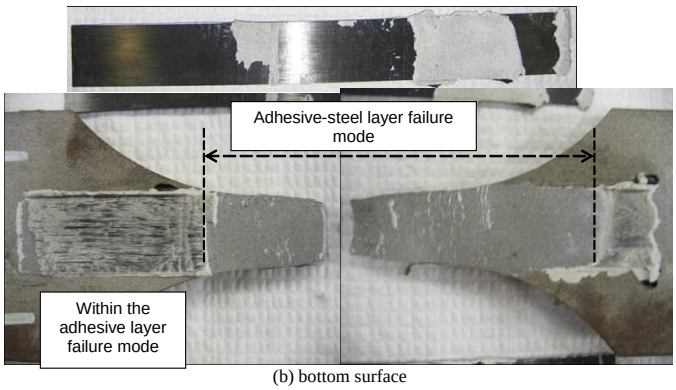

(b) bottom surface

Figure 7. Failure mode of specimen VW1

Sample VW2 was bonded with two layers of 125 mm CFRP on top and bottom faces of the steel plate. The rest of the experimental setup was the same as in sample VW1. Fig. 8 shows the specimen at failure. At the top surface as shown in Fig. 8 (a), the debonding failure occurred on the steel-adhesive layer at the middle part of the steel plate, whereas, CFRP-adhesive layer failure mainly occurred close to the plate end. At the bottom surface, debonding failure occurs at the steel-adhesive layer in the middle of the specimen whereas part of the CFRP plate is still bonded to the steel plate as shown in Fig. 8 (b). The CFRP plate at the top surface debonded at the load of approximately 175 kN. However, the CFRP plate at the bottom surface was still glued onto the steel plate when the steel plate broke.

ISSN XXXX-XXXX

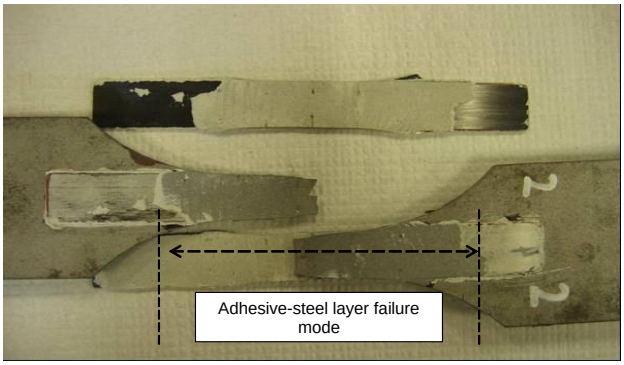

(a) top surface

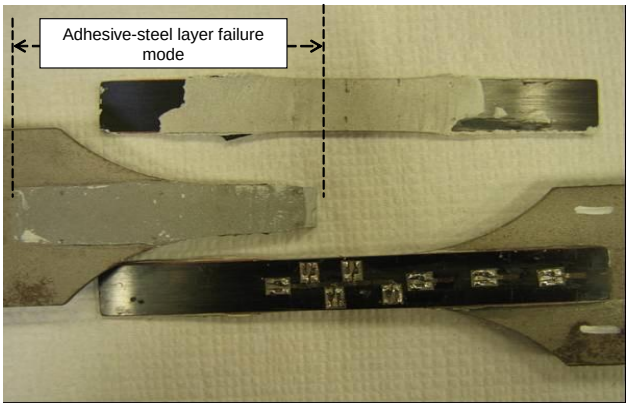

(b) bottom surface

Figure 8. Failure mode of specimen VW2

Fig. 9 shows the experimental and numerical load-strain of steel plate comparison for specimen VW1. The corresponding comparison for load-strain of the CFRP plate is shown in Fig. 10. There are three stages of behaviour experienced by the specimen as illustrated in both figures; linear elastic, steel yielding and debonding. The three behavioural stages of τ-δ relationship in Fig. 1 were correctly predicted by the numerical analysis.

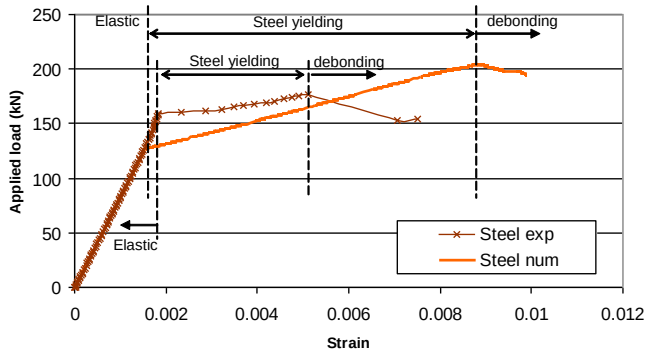

Figure 9. Steel load-strain comparison for VW1

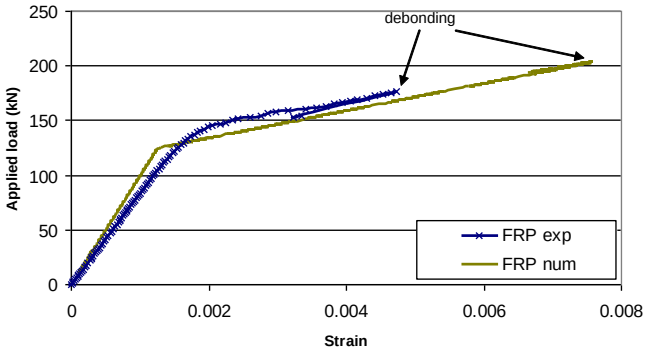

Figure 10. CFRP load-strain comparison for VW1

VI. ANALYSIS OF TEST RESULTS

In this section, the debonding mechanism of CFRP plated steel members is explained when the steel has yielded along the bonded length. For the purpose of demonstrating the debonding mechanism, the CFRP plated steel member with varying widths in Fig. 6 with infinite bond length was used. The values of τ_{max} and δ_{max} used in the numerical analysis were 22.9 MPa and 0.2 mm respectively which was obtained from previous research by the authors (Akbar et al. 2010b).

The slip-strain was calculated from the differences of the steel and CFRP strains. The corresponding slip distribution is shown in Fig. 11. Both figures show that the *slip=slipstrain=0* boundary condition was achieved at the same point at about 200 mm from the middle section. At a lower load (labelled (a)), the slip has just reached its peak value. As the load was increased, the slip at that point increased to (c) as shown in Fig. 11. From the graph it can be observed that the slip increment only occurred at a range from 0 to 200 mm from the middle. The corresponding bond stress distribution in Fig. 12 shows the debonding propagation. At maximum slip, the bond-stress is equal to 0 which is clearly depicted in the graph labelled (a). As the slip keep on increasing, the maximum slip propagates to the left and right ride with the corresponding graph (b) of the bond-stress propagation. The 0 value of bond-stress between the peak bond-stress indicate that debonding has already occurred. From this observation, it can be concluded that debonding starts at the peak slip and then propagates left and right of the bonded length.

ISSN XXXX-XXXX

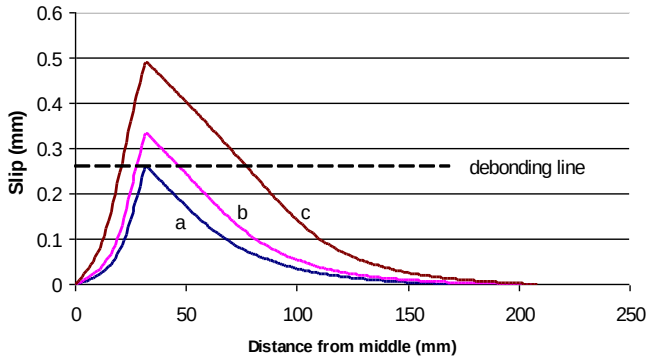

Figure 11. Slip distribution after steel yielding

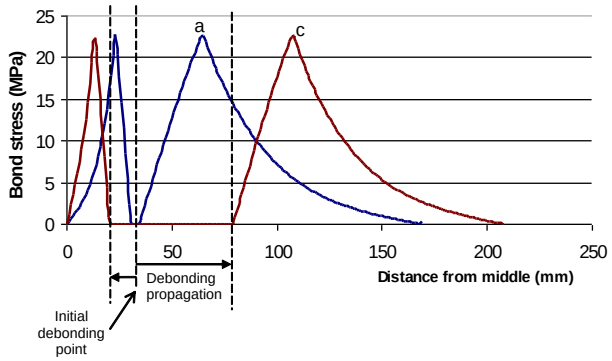

Figure 12. Bond stress distribution after steel yielding

The first debonding mechanism occurred at the plate end whereas the other occurred at the length where the steel has yielded. In the case of plate end debonding, there was a point when the strains in the steel and CFRP were equal which resulted in zero slip-strain and slip. The full description of this behaviour has been described elsewhere (Akbar et al. 2010a). The area where the slip-strain and slip were not zero is shown in the partial interaction region at the right side of Fig. 13.

The second debonding mechanism occurred where the steel has yielded between the plate ends. The point where the slip-strain and slip were zero along the bond length was demonstrated in Figs. 11 and 12 respectively, which was also the boundary condition in the numerical method. Hence, partial interaction region also occurred at the region where the steel has yielded and is shown at the left side of Fig. 13.

The two debonding mechanisms existed at a certain length at which either one of two boundary conditions, σ_p=0 and s=ds/dx=0 are met. These are also the partial interaction regions as shown in Fig. 13. Extending the length of the bond length will only extend the length of the full interaction region.

VII. APPLICATION OF NUMERICAL ANALYSIS

Al-Emrani and Kliger (2006) experimented on CFRP plated tapered steel members with varying CFRP thicknesses. The τ-δ relationship of the adhesive was not available from the published report, hence, the one obtained from this research will be used. Due to this, the objective of this comparison was to analyse the debonding mechanism and not to compare the accuracy of the results in terms of the 'values'. Three specimens were compared, A12, B12 and B17 which have different types of adhesive and CFRP thicknesses. Experimental and FEM results were reported in the published report and reproduced in this section. These published results were then compared with the numerical analyses developed from this chapter.

Fig. 14 shows the comparison of applied load-axial stress from the experiment and numerical analyses on specimen A12 based on the strain readings on the CFRP plate at the middle of the section. According to the experimental report by Al-Emrani and Kliger (2006), specimen A12 failed due to debonding in the middle of specimen after the steel plate yielded.

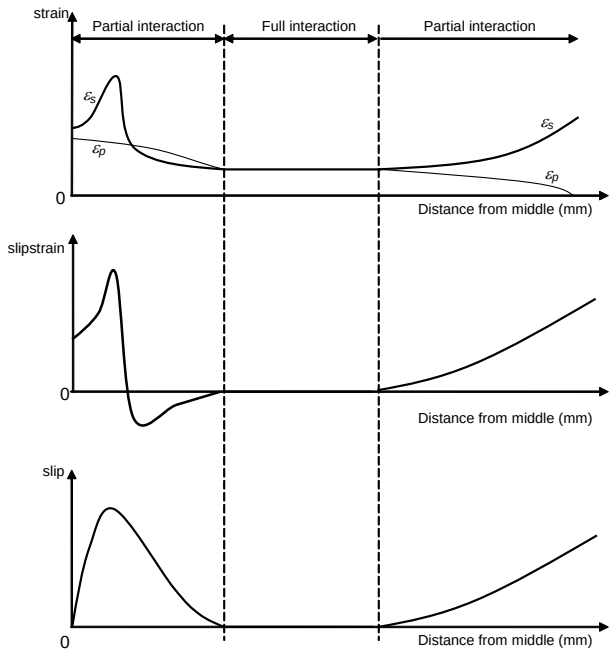

Figure 13 Full and partial interaction regions of CFRP plated steel member

In the numerical analysis, the decrease of the CFRP stresses as shown in Fig. 14 after the steel has yielded suggested that successive yielding of steel leads to the debonding. This is also the type of failure occurred on sample VW1 as reported previously. The stress recorded by the numerical analysis for specimen A12 was 1117 MPa prior to debonding in comparison with 1553 MPa from the experiment. Both values were below the ultimate stress of 1932 MPa, indicating a good correlation by the numerical analysis to predict the failure.

ISSN XXXX-XXXX

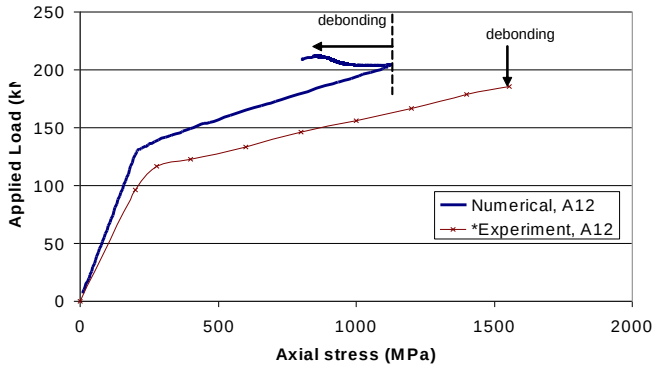

Figure 14 Numerical and experimental load-axial stress comparison for specimen A12

Fig. 15 shows the bond stress distribution along the bonded length from the experiment and numerical for specimen A12. At 150 kN (149 kN for the numerical analysis), the steel plate has yielded, creating a high bond stress at the middle of the specimen. It was suggested by Al-Emrani and Kliger (2006) that debonding may occur first at the middle section before at the plate end based on the high bond stress which also occurred at the plate end. As the applied load increases, the bond stress also increases to the peak, τ_{max}. At this point the slip keeps on increasing while the bond stress begins to drop down to the maximum slip, δ_{max}. Once δ_{max} is reached, no more load can be attained resulting in 0 bond stress as depicted in middle section of the specimen in Fig. 15 for both FEM and numerical analysis. Again this comparison show a good correlation between the FEM carried out by the previous authors and the current research.

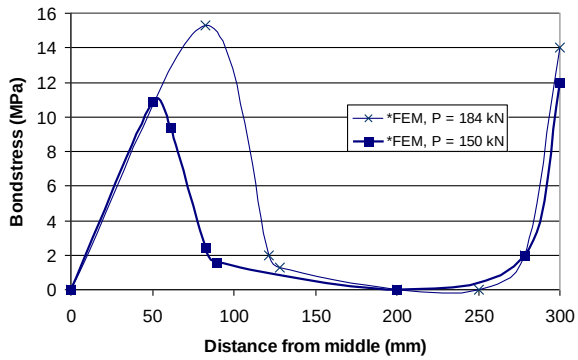

(a) FEM

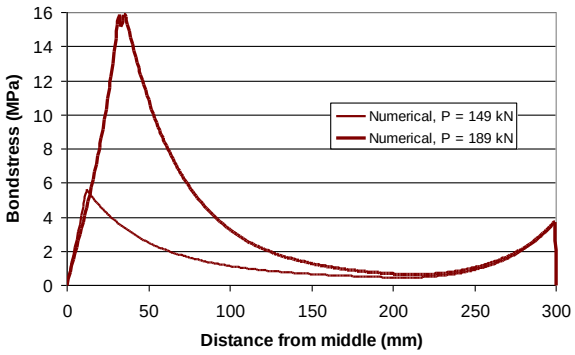

(b) Numerical

Figure 15 Numerical and FEM shear stress comparison across the bonded length.

VIII. CONCLUSIONS

A numerical method was developed to study the debonding mechanism of CFRP plated steel members based on partial and full interaction theory. This numerical method was able to show the debonding mechanism for debonding due to the yielding of steel. The numerical analysis results were compared with the experiments conducted and the published experiment. From this study, it can be concluded that if the steel yielded between the plate ends, the huge difference of steel and CFRP strains will create huge slip with subsequent debonding. This will results in the debonding to start at the location where the steel has yielded and then propagate towards the middle section and the plate ends.

ACKNOWLEDGMENT

The authors would like to extend their acknowledgement to the Universiti Teknologi PETRONAS and The University of Adelaide for providing the funding and resources for the accomplishments of this research study.

REFERENCES

Akbar, I., Oehlers, D. J., and Ali, M. S. M. (2010a). "Partial and Full Interaction Behaviour of FRP Plated Steel Member." International Conference on Sustainable Building and Infrastucture, Kuala Lumpur.

Akbar, I., Oehlers, D. J., and M.S., M. A. (2010b). "Derivation of the bond-slip characteristics for FRP plated steel members." *Journal of Constructional Steel Research*, 66(8-9), 1047-1056

Al-Emrani, M., and Kliger, R. (2006). "Experimental and numerical investigation of the behaviour and strength of composite steel-CFRP members." *Advances in Structural Engineering*, 9(6), 819-831.

Al-Saidy, A. H., Klaiber, F. W., and Wipf, T. J. (2005). "Strengthening of steel–concrete composite girders using carbon fiber reinforced polymer plates." *Construction and Building Materials*, 21(2), 295-302.

Buyukozturk, O., Gunes, O., and Karaca, E. (2003). "Progress on understanding debonding problems in reinforced concrete and steel members strengthened using FRP composites." *Construction and Building Materials*, 18(1), 9-19.

Haskett, M., Oehlers, D. J., and Ali, M. S. M. (2007). "Local and global bond characteristics of steel reinforcing bars." *Engineering Structures*, 30(2), 376-383.

Sebastian, W. M. (2003b). "Nonlinear proportionality of shear-bond stress to shear force in partially plastic regions of asymmetric FRC-laminated steel members." *International Journal of Solids and Structures*, 40(1), 25-46.

Seracino, R., Raizal Saifulnaz, M. R., and Oehlers, D. J. (2007). "Generic Debonding Resistance of EB and NSM Plate-to-Concrete Joints." *Composite for Constructions*, 11(1), 62-70.

Xia, S. H., and Teng, J. G. (2005). "Behaviour of FRP-to-steel bonded joints." Proceedings of the International Symposium on Bond Behaviour of FRP in Structures, J. F. Chen and J. G. Teng, eds., International Institute for FRP in Construction, Hong Kong, 419-426.

Yuan, H., Teng, J. G., Seracino, R., Wu, Z. S., and Yao, J. (2004). "Full-range behavior of FRP-to-concrete bonded joints." *Engineering Structures*, 26(5), 553-565.

Zhao, X.-L., and Zhang, L. (2007). "State-of-the-art review on FRP strengthened steel structures." *Engineering Structures*, 29(8), 1808-1823.